

## RESEARCH ARTICLE

# Inhibition of cancer cell proliferation by adenosine triphosphate-triggered codelivery system of p53 gene and doxorubicin

Yong Liu, Xinxin Shao, Zhiyuan Shi, Quanshun Li\*

Key Laboratory for Molecular Enzymology and Engineering of Ministry of Education, School of Life Sciences, Jilin University, Changchun 130012, China

**Received:** May 17, 2019  
**Accepted:** June 13, 2019  
**Published Online:** June 25, 2019

### \*CORRESPONDENCE TO

Quanshun Li, Key Laboratory for Molecular Enzymology and Engineering of Ministry of Education, School of Life Sciences, Jilin University, Changchun 130012, China.  
**Tel.:** +86-431-85155201  
**Fax:** +86-431-85155200  
**Email:** quanshun@jlu.edu.cn

### CITATION

Liu Y, Shao X, Shi Z, Li Q. Inhibition of cancer cell proliferation by adenosine triphosphate-triggered codelivery system of p53 gene and doxorubicin. *Cancer+*, 1(2):3-11. doi: 10.18063/cp.v1i2.239

**Copyright:** © 2019. Liu Y, Shao X, Shi Z, Li Q. This is an Open Access article distributed under the terms of the Creative Commons Attribution-NonCommercial 4.0 International License (<http://creativecommons.org/licenses/by-nc/4.0/>), permitting all noncommercial use, distribution, and reproduction in any medium, provided the original work is properly cited.

**Abstract:** The codelivery of drugs and genes by stimuli-responsive nanocarriers is a promising strategy for achieving an effective cancer treatment. In this study, an adenosine triphosphate (ATP)-responsive nanosystem was constructed to codeliver doxorubicin (DOX) and p53 gene based on an ATP-triggered aptamer and polyethyleneimine (PEI). In this system, DOX interacts with the GC-rich motif of duplex formed by the aptamer and its cDNA sequence. Then, a ternary nanocomplex DOX-Duplex/PEI/p53 was constructed using cationic carrier PEI25K for facilitating the intracellular delivery and release of p53 gene and DOX. The DOX-Duplex/PEI/p53 nanocomplex was found to possess an efficient anticancer effect, which was attributed to the ability of the system to trigger cell apoptosis and meanwhile block the cell cycle at G2 phase. The favorable antiproliferative effect was found to be associated with the rapid DOX and p53 gene release in response to the intracellular ATP concentration and the synergistic effect of therapeutic drug and gene.

**Keywords:** adenosine triphosphate-responsive aptamer; doxorubicin; p53 gene; codelivery; synergistic effect

## 1. Introduction

In recent years, chemotherapy has emerged as the most common strategy for cancer treatment<sup>[1]</sup>. However, the application of chemotherapy was strictly hindered by its undesirable side effects, low antitumor efficiency, and strong drug resistance<sup>[2,3]</sup>. On the contrary, gene therapy has many advantages since it is capable of altering the mutated genes or their expression level to manipulate the proliferative effect of cancer cells by delivering therapeutic genes<sup>[4]</sup>, and thus, it has been widely accepted as an efficient approach in the cancer treatment. Among therapeutic genes, p53 gene is a famous tumor suppressor which has been widely investigated, as it exhibits a great potential in inhibiting the tumor growth by multiple pathways including the induction of cell cycle arrest and cell apoptosis<sup>[5,6]</sup>.

At present, the combination therapy based on the codelivery of chemotherapeutics and genes by nanocarriers has been proposed to achieve an excellent antitumor effect with the advantages of lower drug dosage and limited toxicity<sup>[7,8]</sup>. To enhance the therapeutic efficacy of the codelivery systems, various intelligent nanocarriers have been purposely developed to facilitate the accumulation of nanocarriers at the tumor site and accelerate the intracellular release of payloads in response to different stimulus such as pH<sup>[9]</sup>, enzymes<sup>[10]</sup>, light<sup>[11]</sup>, temperature<sup>[12]</sup>, and intracellular reduction conditions<sup>[13]</sup>. However, these stimuli-

responsive nanocarriers require complicated design and construction procedures which are easily affected by the external factors<sup>[14,15]</sup>.

In cancer cells, the extracellular concentration of adenosine triphosphate (ATP) was much lower (<0.4 mM) than that in the intracellular environment (ca. 1–10 mM), thereby providing a feasible condition for the construction of intelligent nanomaterials in response to ATP stimuli<sup>[16,17]</sup>. Recently, an ATP-responsive nanomaterial composed of an ATP-binding aptamer and its complementary chain (cDNA) has been successfully developed for the loading and release of doxorubicin (DOX)<sup>[18,19]</sup>. In this ATP-triggered system, DOX was integrated into the double-stranded duplex in a low ATP concentration due to the introduction of high GC content and then triggered to be released in response to high intracellular ATP status. Since the aptamers are easily degraded by nucleases in the circulation, an efficient carrier is highly required for the stable delivery of aptamers. In recent years, branched polyethyleneimine (PEI) (molecular weight of 25 kDa, PEI25K) has been widely regarded as a “gold standard” in the polycation carriers-mediated gene delivery, which can form a stable nanoparticle with nucleic acids and achieves the endo/lysosomal escape through the “proton sponge” effect to prevent the degradation of nucleic acids in the acidic environment<sup>[20,21]</sup>.

In the present study, the codelivery of p53 gene and DOX was realized on the basis of an ATP-triggered aptamer and its cDNA sequence, using PEI25K as a carrier. In this system, PEI25K could efficiently form a stable nanocomplex with DOX-loaded aptamer and p53 gene and further protect nucleic acids from the degradation by nucleases. Finally, the antitumor response in human prostate cancer cell line PC-3 was evaluated to analyze the synergistic effect of p53 gene and DOX.

## 2. Materials and Methods

### 2.1. Materials

PEI25K, 3-(4,5-dimethylthiazol-2-yl)-2,5-diphenyltetrazolium bromide (MTT), and heparin were provided by Sigma-Aldrich (St. Louis, MO). Doxorubicin hydrochloride (DOX, >98%) was obtained from Beijing HVSF United Chemical Materials Co., Ltd. (Beijing, China). PI-based cell cycle and Annexin V-FITC/PI-based apoptosis detection kits were obtained from Bestbio (Shanghai, China). Dulbecco's Modified Eagle's Medium (DMEM) and fetal bovine serum (FBS) were provided by Gibco (Grand Island, MO). Phosphate-buffered saline (PBS) and polyvinylidene fluoride (PVDF) membrane were obtained from Amresco (Solon, OH) and Millipore (Billerica, MA), respectively. Antibodies against p53 and procaspase-3 were purchased from Abcam (Shanghai, China). The BCA protein assay kit was purchased from Promega (Madison, WI). The activities of caspases-3, -8, and -9 were detected by commercially available kits obtained from Promega (Madison, WI). All

other reagents were purchased and used without further purification.

The ATP-responsive aptamer and its complementary DNA (cDNA) were synthesized by Sangon Biotech (Shanghai, China). The sequence of aptamer and cDNA was listed below:

Aptamer: 5'-ACC TGG GGG AGT ATT GCG GAG GAA GGT-3';

cDNA: 5'-ACC TTC CTC CGC AAT ACT CCC CCA GGT-3'.

### 2.2. Preparation and characterization of DOX-Duplex/PEI/p53 nanocomplex

The DOX-Duplex was constructed in accordance with the previously reported method<sup>[18]</sup>. In brief, the duplex complex was prepared by the incubation of ATP-responsive aptamer solution (20 μM) and its cDNA at room temperature for 45 min. After the addition of DOX solution (20 μM) in the duplex complex dropwise, the DOX-Duplex complex was constructed during the incubation of the mixture at room temperature for 15 min. The DOX-Duplex complex was then incubated in different ATP solutions (0.4 or 4.0 mM) to determine the DOX loading and release profile through the fluorescence intensity of DOX. For the preparation of DOX-Duplex/PEI/p53 nanocomplex, p53 gene was first mixed with DOX-Duplex complex, and the obtained sample was mixed with PEI25K at different mass ratios. After settling down the sample at room temperature for 30 min, Nano ZS90 Zetasizer (Malvern Instrument, UK) was used to evaluate the average particle size and zeta potential values of DOX-Duplex/PEI/p53 nanoparticles.

### 2.3. Gel retardation assay of DOX-Duplex/PEI/p53 nanocomplex

The gel retardation assay was employed to characterize the condensing capacity of PEI25K to DOX-Duplex and p53, in which the formed nanocomplexes were subjected to 1% agarose gel electrophoresis (20 min, 120 V). Further, the stability of nanocomplexes was monitored throughout the period of incubation with DNase I at 37°C for 3 h, and the heparin solution (4 mg/mL) was adopted to trigger the p53 gene release from nanocomplexes. Similarly, the products were electrophoresed on 1% agarose gel as described above.

### 2.4. Cellular uptake of DOX-Duplex/PEI/p53 nanocomplex

The PC-3 cells were inoculated at an initial density of  $2.5 \times 10^5$  cells/well in 6-well plates and cultured overnight. Then, the cells were incubated with DOX-Duplex/PEI/p53 nanocomplex in serum-free medium for 6, 12, 18, and 24 h, respectively, and observed by an IX71 fluorescence microscopy (Olympus, Tokyo, Japan).

## 2.5. Cytotoxicity assay of ternary nanocomplex

The cytotoxicity assay of Duplex/PEI/green fluorescent protein (GFP) ternary nanocomplex was conducted through MTT method using PC-3 cells. Briefly, the cells were inoculated into 96-well plates ( $7.0 \times 10^3$  cells/well) and incubated overnight. After removing the medium from each well, the serum-free DMEM harboring the corresponding nanocomplexes (100  $\mu$ L) was added into each well and the cells were incubated for 24 h. At the end of the incubation, MTT solution (20  $\mu$ L, 5 mg/mL) was used to treat the samples in each well for 4 h. Following the removal of medium, the formazan crystal formed in each well was dissolved using 150  $\mu$ L of dimethyl sulfoxide. GF-M3000 microplate reader (Shandong, China) was used to measure the absorbance of the dissolved formazan crystal at 492 nm. The cell viability was calculated by the ratio of absorbance of the treated and control cells.

## 2.6. Cell apoptosis assay induced by DOX-Duplex/PEI/p53 nanocomplex

The PC-3 cells were inoculated into 6-well plates ( $2.0 \times 10^5$  cells/well) and incubated overnight. After removing the medium, 2 mL of serum-free DMEM containing different nanocomplexes were added into each well. Followed by the incubation for 6 h, the cells were cultured by fresh medium supplemented with 10% FBS for an additional 24 h. The treated cells were collected and stained with the solutions provided in the detection kit based on the manufacturer's instructions, and FACSCalibur (BD Biosciences, San Jose, CA) was employed to measure the apoptotic ratio.

## 2.7. Cell cycle arrest assay induced by DOX-Duplex/PEI/p53 nanocomplex

The cell culture and transfection procedures were described in section 2.6. Subsequently, the harvested cells were subjected to fixation in 75% ethanol at 4°C overnight and rinsed with cold PBS for 3 times. The fixed cells were incubated with RNase A solution (20  $\mu$ L) at 37°C for 30 min and then stained with PI solution (300  $\mu$ L) at 4°C for 1 h in the dark. Finally, FACSCalibur (BD Biosciences, San Jose, CA) was employed to analyze the cell cycle.

## 2.8. Western blotting assay

The cell culture and the treatment with DOX-Duplex/PEI/p53 nanocomplex were performed as described in section 2.6. After the transfection with different nanocomplexes, the collected cells were lysed with RIPA buffer with 1 mM phenylmethanesulfonyl fluoride and quantified by BCA protein kit. An equal quantity of supernatant proteins was used for 12% sodium dodecyl sulfate-polyacrylamide gel electrophoresis and transferred to PVDF membrane through electroblotting. To block the non-specific binding, the PVDF membrane was treated with 5% skim milk for

2 h. The membrane was subjected to the incubation with individual primary antibodies at 4°C overnight and the horseradish peroxidase-conjugated secondary antibody at room temperature for an additional 1 h. The enhanced chemiluminescent solution was used to visualize the PVDF membrane. The protein expression level was identified using  $\beta$ -actin as a control.

## 2.9. Activity assays of caspase-3, -8, and -9

The cell treatment procedures were described in section 2.6. After the treated cells were incubated with 100  $\mu$ L of lysis buffer, the supernatant was harvested by centrifuging at 12,000 rpm for 15 min and quantified by BCA protein kit. Finally, according to the instructions, the activities of caspase-3, -8, and -9 were measured through the incubation of the equal amount of supernatant and individual substrate in the corresponding activity assay kits.

## 3. Results and Discussion

### 3.1. Preparation and characterization of DOX-Duplex/PEI/p53 nanocomplex

The fluorescence intensity of DOX-Duplex and DOX was first detected to confirm whether DOX was loaded in the duplex formed by the ATP aptamer and its cDNA. A strong fluorescence intensity at 570 nm was clearly observed in free DOX while the fluorescence dramatically decreased in DOX-Duplex [Figure 1A], which was attributed to the resonance energy transfer generated by the insertion of DOX into the duplex chain. To investigate the ATP-dependent DOX release behavior, DOX-Duplex was incubated with different ATP concentrations to mimic the intracellular and extracellular environments. The previous reports have demonstrated that the extracellular ATP concentration (<0.4 mM) is much lower than that in the cytosol (1–10 mM)<sup>[22-25]</sup>. Thus, 0.4 mM and 4.0 mM of ATP concentrations were used to mimic the corresponding ATP concentrations in the extracellular and intracellular environments, respectively. As shown in Figure 1B, limited DOX release was observed when DOX-Duplex was treated with 0.4 mM ATP. Notably, DOX release was efficiently triggered at a higher concentration of ATP (4.0 mM), indicating that DOX-Duplex could induce the DOX release in an ATP-triggered manner. Meanwhile, the system could obtain a favorable intracellular ATP response, and thus, it was favorable for achieving high antitumor efficacy.

Subsequently, PEI25K was used as a cationic carrier for the delivery of p53 gene and DOX-Duplex. The condensation ability of PEI25K for DOX-Duplex was investigated through gel retardation assay. As indicated in Figure 2A, obvious retardation was achieved at the mass ratio of >0.5, suggesting that the aptamer duplex was efficiently condensed by PEI25K into stable nanoparticles. Moreover, PEI25K maintained the favorable binding and condensation ability for the

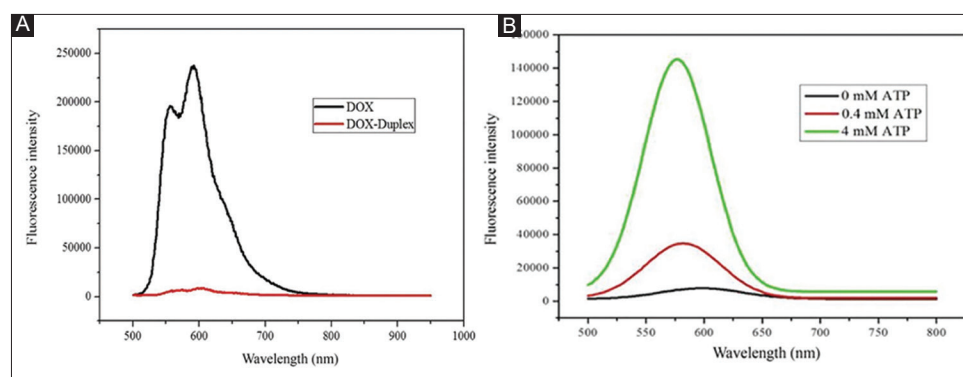


**Figure 1.** The fluorescence intensity of doxorubicin (DOX) and DOX-Duplex (A). The DOX release profile from DOX-Duplex with the treatment with 0, 0.4, and 4.0 mM ATP, respectively (B).

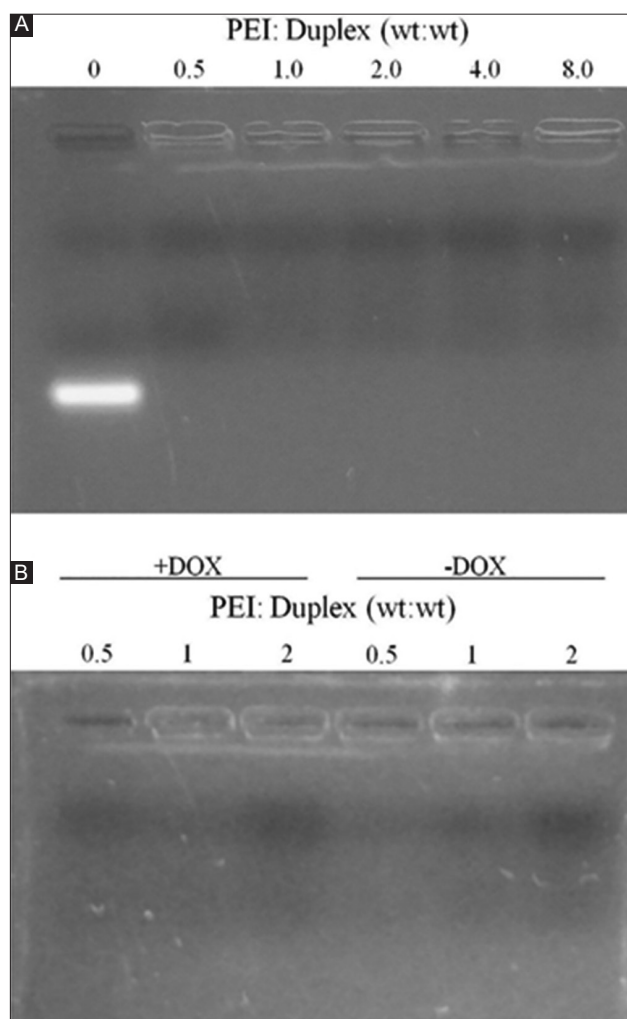


**Figure 2.** Gel retardation assay of polyethyleneimine (PEI)/duplex nanocomplex at different mass ratios (A). Influence of doxorubicin on the stability of PEI/duplex nanocomplex (B).

aptamer duplex in the presence or absence of DOX molecules, as complete retardation was maintained for all the groups [Figure 2B]. Further, to measure the binding and condensation capability of PEI25K for both p53 gene and DOX-Duplex, gel retardation assay was performed.

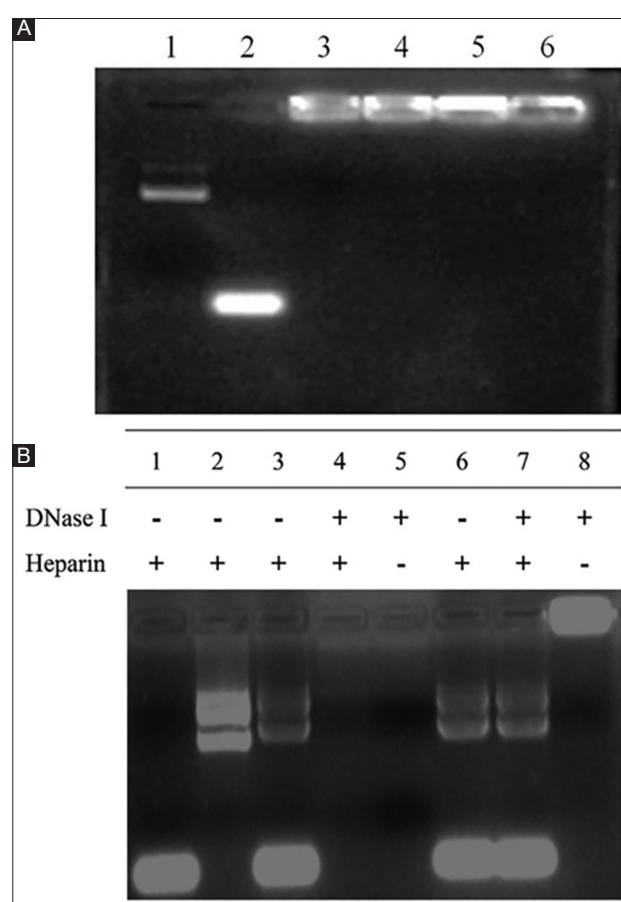


**Figure 3.** (A) Gel retardation assay of doxorubicin (DOX)-Duplex/polyethyleneimine/p53 nanocomplex at different mass ratios. Lane 1: Free p53 gene, lane 2: Free DOX-Duplex, lane 3-8: DOX-Duplex/PEI/p53 nanocomplex at mass ratios of 1:1:1, 1:2:1, 1:4:1, and 1:8:1, respectively. (B) Agarose gel electrophoresis for analyzing the stability of DOX-Duplex/PEI/p53 nanocomplex in the presence of DNase I. Lane 1: Free p53 gene; lane 2: DOX-Duplex, lane 3-5: DOX-Duplex/p53 nanocomplex, and lane 6-8: DOX-Duplex/PEI/p53 nanocomplex.

As shown in Figure 3A, compared with p53 plasmid and DOX-Duplex, the DOX-Duplex/PEI/p53 ternary nanocomplex was completely retarded at the mass ratio



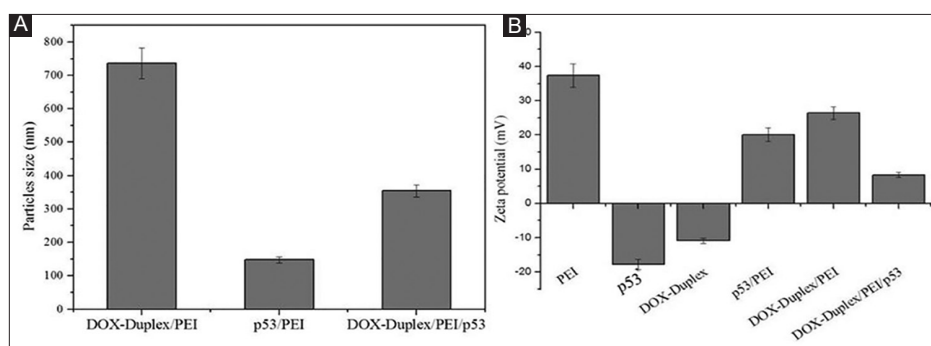


**Figure 4.** The hydrodynamic diameter (A) and zeta potential (B) values of nanocomplexes.

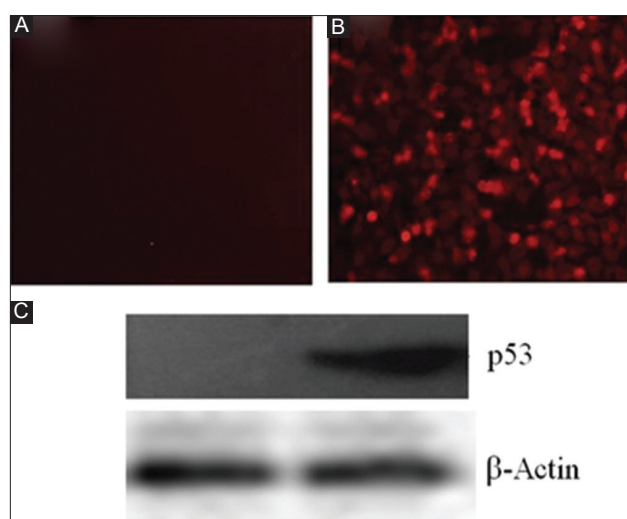


**Figure 5.** The endocytosis analysis of doxorubicin (DOX)-Duplex/polyethyleneimine (PEI)/p53 nanocomplex through the fluorescence microscopy: (A) The control group. (B) DOX-Duplex/PEI/p53 nanocomplex. (C) The expression level of p53 protein in PC-3 cells after the treatment of DOX-Duplex/PEI/p53 nanocomplex for 24 h. Left panel: Control group; right panel: DOX-Duplex/PEI/p53 nanocomplex.

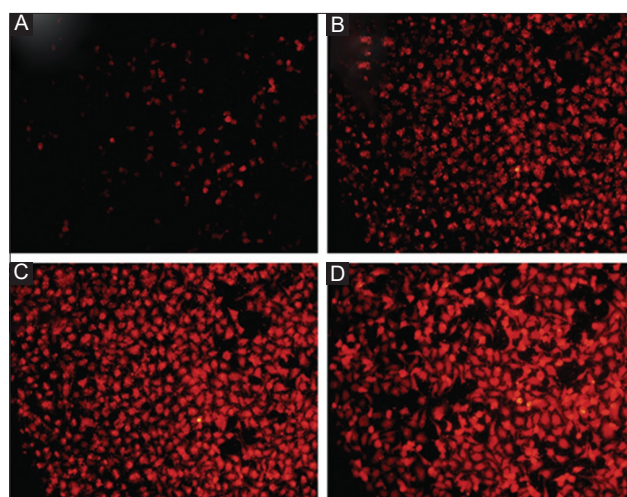


**Figure 6.** The doxorubicin (DOX) release profile of DOX-Duplex/polyethyleneimine/p53 nanocomplex after the transfection for 6 (A), 12 (B), 18 (C), and 24 h (D), respectively.

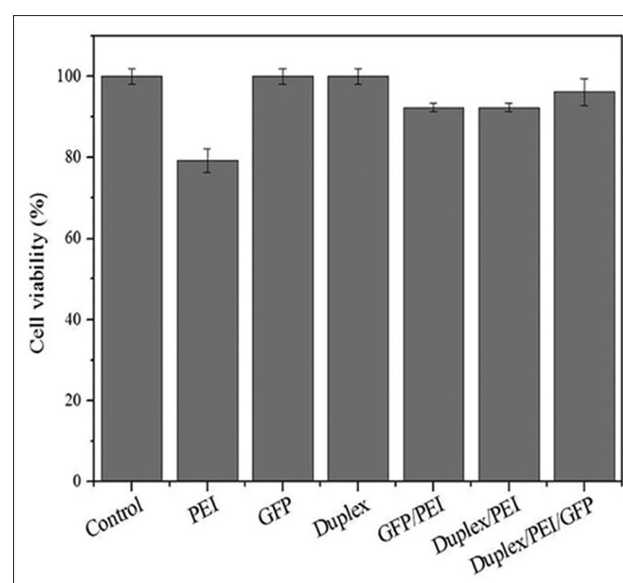


**Figure 7.** The cytotoxicity analysis of the ternary nanocomplex duplex/polyethyleneimine/green fluorescent protein.

of 1:1:1, which indicates a superior condensing ability of PEI25K for these two components. Then, we evaluated the protective effect of PEI25K for these two components against the DNase I treatment through agarose gel electrophoresis [Figure 3B]. Apparently, free p53 plasmid and DOX-Duplex were easily degraded by DNase I. In contrast, obvious bands of p53 plasmid and DOX-Duplex were detected after the DNase I digestion in the DOX-Duplex/PEI/p53 group, demonstrating that PEI25K could protect p53 plasmid and DOX-Duplex from the DNase I degradation.

The characterization of size and zeta potential values of nanocomplexes was further conducted. As shown in Figure 4A, DOX-Duplex/PEI nanocomplex exhibited a much larger hydrodynamic diameter (736.5 nm), which could be caused by the decreased electrostatic interaction induced by the presence of DOX in DOX-Duplex. Notably, compared with DOX-Duplex/PEI nanocomplex, the ternary nanocomplex DOX-Duplex/PEI/p53 showed a relatively smaller size (354.4 nm). These results were mainly caused by that the addition

of plasmid in the nanocomplex could provide a stronger electrostatic interaction with PEI25K, thereby leading to a more condensed structure. Meanwhile, DOX-Duplex/PEI/p53 complex showed a positively charged state with the zeta potential value of 7.9 mV [Figure 4B], which could be suitable for the cellular uptake of nanoparticles through the interaction with negatively charged cell membrane.

### 3.2. Cellular uptake of DOX-Duplex/PEI/p53 nanocomplex

The endocytosis behavior of DOX-Duplex/PEI/p53 nanocomplex was then studied using PC-3 cell line as a model. As demonstrated in Figure 5A and B, compared with the control group, an obvious red fluorescence was observed in DOX-Duplex/PEI/p53 group after the incubation for 6 h, indicating that the nanocomplex

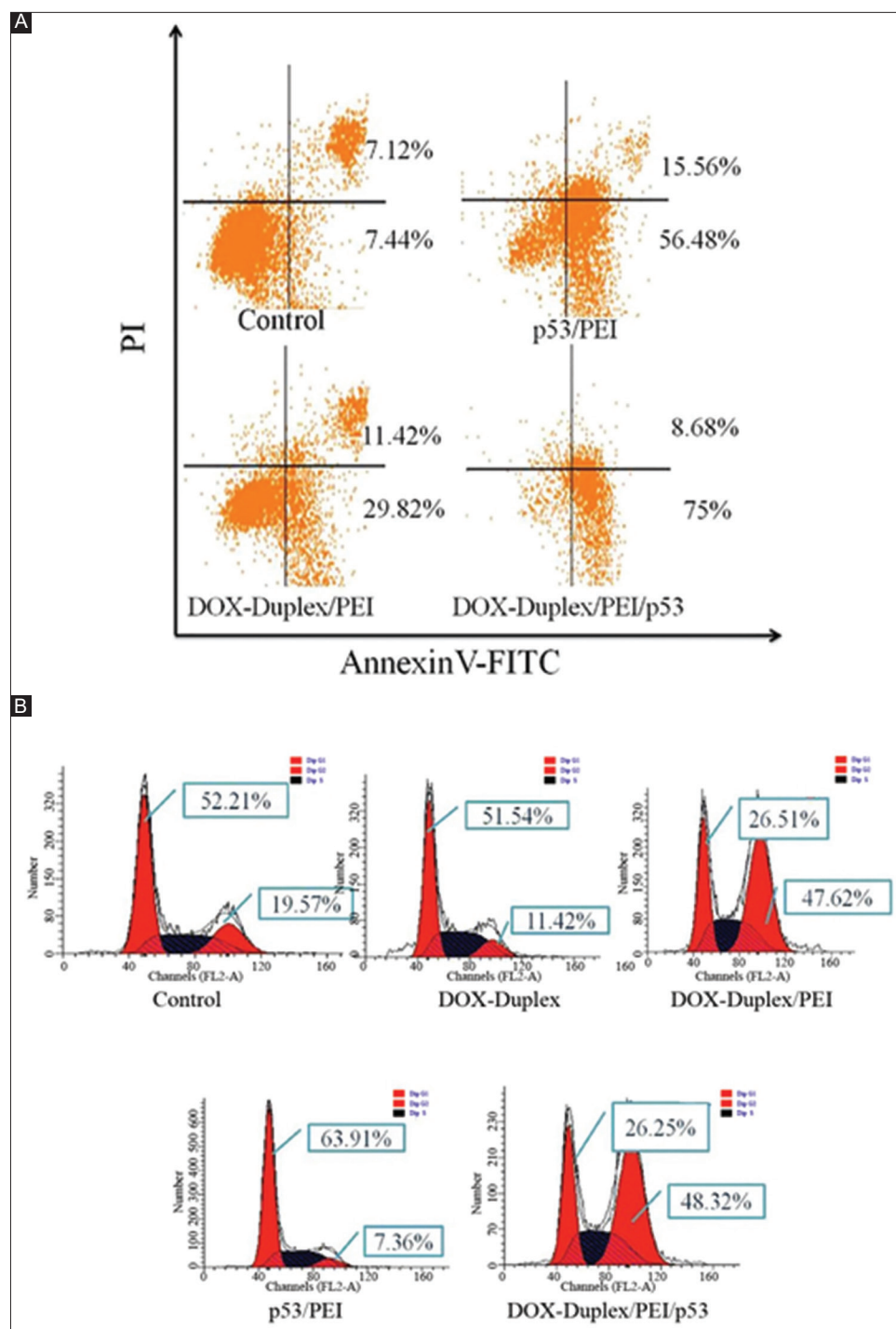


**Figure 8.** The cell apoptosis (A) and cell cycle (B) analysis of PC-3 cells after the treatment with different nanoparticles.

successfully achieved the intracellular delivery of DOX. Meanwhile, to detect the expression level of p53 protein and further identify the successful transfection of p53 gene, we conducted Western blotting analysis after the cells were treated with the ternary nanocomplex. Compared to the p53-null state of PC-3 cells, the expression of p53 protein could be clearly increased after the transfection [Figure 5C], providing direct evidence that DOX-Duplex/PEI/p53 nanocomplex could mediate the delivery of p53 gene into the cancer cells and further facilitate the expression of therapeutic gene. Further, the DOX release profile of ternary nanocomplex was detected at 6, 12, 18, and 24 h, respectively. Apparently, the red fluorescence intensity was gradually increased with the increasing treatment time [Figure 6], revealing that the release of DOX was conducted in a time-dependent manner. In this regard, DOX-Duplex/PEI/p53 nanocomplex could induce the controlled release of DOX, which was potential in the reduction of systemic toxicity in future applications. In summary, DOX-Duplex/PEI/p53 nanocomplex efficiently mediated the *in vitro* codelivery of DOX and p53 gene and also triggered the DOX release in an ATP-responsive and time-dependent pattern.

### 3.3. Antiproliferative analysis of DOX-Duplex/PEI/p53 nanocomplex

The cytotoxicity of ternary nanocomplex was investigated through MTT assay using duplex and/or GFP plasmid as models. As shown in Figure 7, PEI25K exhibited an obvious cytotoxicity due to its excessive positive charge. Interestingly, compared with free PEI25K, both binary nanocomplex and ternary nanocomplex exhibited a reduced cell cytotoxicity, which could be attributed to the neutralization of positive charge by GFP plasmid and duplex.

Subsequently, we detected the cell apoptotic effect induced by DOX-Duplex/PEI/p53 nanocomplex through flow cytometry. In comparison to the untreated cells, an evident early apoptosis was obtained after the treatment with p53/PEI and DOX-Duplex/PEI with ratios of 56.5% and 29.8% [Figure 8A], indicating that PEI25K was capable of delivering p53 gene or DOX-Duplex into cancer cells and triggered the cell apoptosis. Notably, the cells treated with DOX-Duplex/PEI/p53 nanocomplex possessed the highest ratio of early apoptosis (75.0%), much higher than those of p53/PEI and DOX-Duplex/PEI groups, suggesting DOX-Duplex/PEI/p53 nanocomplex induced an obvious cell apoptosis through the synergistic effect of p53 gene and DOX. To obtain a detailed mechanism of apoptosis induced by DOX-Duplex/PEI/p53 nanocomplex, we detected the expression level of procaspase-3 through Western blotting analysis [Figure 9A]. Clearly, the procaspase-3 expression was remarkably reduced after the transfection of ternary nanocomplex, indicating the activation of caspase-3 by the cleavage of its precursor procaspase-3. Consistently, the activity of caspase-3 was sharply increased after the

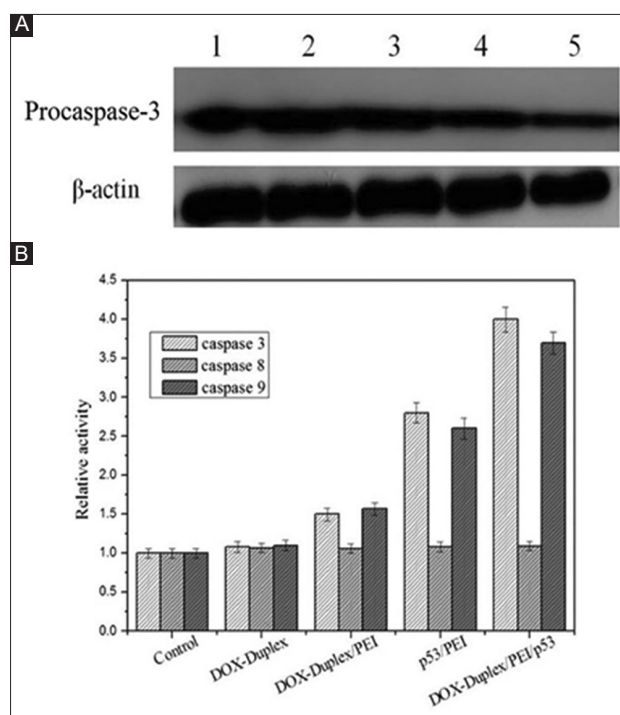


**Figure 9.** (A) The procaspase-3 expression level after the transfection of different nanocomplexes. Lane 1: Control, lane 2: Doxorubicin (DOX)-Duplex, lane 3: DOX-Duplex/polyethylenimine, lane 4: p53/PEI, and lane 5: DOX-Duplex/PEI/p53. (B) The activities of caspase-3, -8, and -9 after the transfection of different nanocomplexes.

treatment with DOX-Duplex/PEI/p53 nanocomplex, as shown in Figure 9B. The caspase-3 activation has been regarded as a critical factor in the caspase family-based apoptosis signaling pathway. Thus, our results clearly demonstrated that the transfection of ternary nanocomplex could obviously activate the caspase-3-mediated apoptotic cascade. In addition, the caspase-9 activity was increased in DOX-Duplex/PEI/p53 nanocomplex group while the activity of caspase-8 did not change, indicating that DOX-Duplex/PEI/p53 nanocomplex triggered the cell apoptosis through the mitochondria-dependent apoptotic route.

Besides, we also conducted the cell cycle analysis using flow cytometry to determine whether the inhibition of cell proliferation was induced by the cell cycle arrest. In comparison to the untreated cells, free DOX-Duplex was not capable of inducing any cell cycle arrest [Figure 8B]. Nevertheless, the population of cells arrested at G2 phase was sharply increased when cells were treated with DOX-Duplex/PEI nanocomplex (47.6%), indicating that PEI25K efficiently mediated the intracellular delivery of DOX-Duplex and triggered the cytosolic release of DOX to block the cell cycle at G2 phase. Further, the p53/PEI nanocomplex improved the ratio of G1 phase, suggesting that the transfection of p53 gene manipulated the cell cycle arrest at G1 phase which was an intrinsic characteristic of p53 gene. These results were consistent with our previous



reports that DOX-Duplex could achieve the cell cycle arrest at G2 phase in HepG2 cells<sup>[16]</sup>, and PEI-mediated p53 gene delivery could block the cell cycle at G1 phase in HeLa and PC-3 cells<sup>[20]</sup>. Notably, the ternary nanocomplex DOX-Duplex/PEI/p53 demonstrated an obvious G2 phase arrest (48.3%), which could mainly be relied on the stronger arrest at G2 phase induced by DOX-Duplex. Taken together, the DOX-Duplex/PEI/p53 complex exhibited an obvious antiproliferative effect on cancer cells through triggering cell cycle arrest at G2 phase and apoptotic effect.

## 4. Conclusion

In the present study, we developed an ATP-responsive nanocarrier for realizing the codelivery of p53 gene and DOX through an ATP-triggered aptamer and PEI25K. The nanocarrier was demonstrated to efficiently achieve the anticancer effect through blocking the cell cycle at G2 phase and triggering the cell apoptosis, which was caused by the rapid DOX and p53 gene release in the response to intracellular ATP environment and the synergistic effect between DOX and p53 gene. Therefore, the nanocarrier based on the ATP-triggered aptamer was potentially to be used as a system for codelivering the therapeutic drugs and genes, providing a promising strategy for the cancer treatment.

## 5. Acknowledgments

The research was supported by National Key R&D Program of China (2018YFC1105401), National Natural Science Foundation of China (81673502 and 81872928), Province-University Cooperation Project of Jilin Province (SXGJQY2017-4), Science and Technology Department of Jilin Province (20190201288JC), and Education Department of Jilin Province (JJKH20190010KJ).

## 6. Authors' Contributions

Y.L. and Q.L. designed the experiments and wrote and revised the paper. Y.L., X.S., and Z.S. conducted the experiments and data analysis.

## Conflicts of Interest

The authors declare no potential conflicts of interest.

## References

- Gandhi L, Rodriguez-Abreu D, Gadgeel S, *et al.*, 2018, Pembrolizumab Plus Chemotherapy in Metastatic Non-small-cell Lung Cancer. *N Engl J Med*, 378:2078-92. DOI 10.1056/NEJMoa1801005.
- Benoist S, Nordlinger B, 2009, The Role of Preoperative Chemotherapy in Patients with Resectable Colorectal Liver Metastases. *Ann Surg Oncol*, 16:2385-90. DOI 10.1245/s10434-009-0492-7.
- Dean M, Fojo T, Bates S, 2005, Tumour Stem Cells and Drug Resistance. *Nat Rev Cancer*, 5:275-84. DOI 10.1038/nrc1590.
- Naldini L, 2015, Gene Therapy Returns to Centre Stage. *Nature*, 526:351-60. DOI 10.1038/nature15818.
- Schuler M, Herrmann R, de Greve J L, *et al.*, 2001, Adenovirus-mediated Wild-Type p53 Gene Transfer in Patients Receiving Chemotherapy for Advanced Non-small-cell Lung Cancer: Results of a Multicenter Phase II Study. *J Clin Oncol*, 19:1750-8. DOI 10.1200/JCO.2001.19.6.1750.4
- Swisher SG, Roth JA, Komaki R, *et al.*, 2003, Induction of p53-regulated Genes and Tumor Regression in Lung Cancer Patients after Intratumoral Delivery of Adenoviral p53 (INGN 201) and Radiation Therapy. *Clin Cancer Res*, 9:93-101.
- Wang Y, Gao S, Ye WH, *et al.*, 2006, Co-delivery of Drugs and DNA from Cationic Core-shell Nanoparticles Self-assembled from a Biodegradable Copolymer. *Nat Mater*, 5:791-6. DOI 10.1038/nmat1737.
- Wei R, Cheng L, Zheng M, *et al.*, 2012, Reduction-responsive Disassemblable Core-cross-linked Micelles Based on Poly(ethylene glycol)-b-poly(N-2-hydroxypropyl methacrylamide)-lipoic Acid Conjugates for Triggered Intracellular Anticancer Drug Release. *Biomacromolecules*, 13:2429-38. DOI 10.1021/bm3006819.
- Yang Q, Wang S, Fan P, *et al.*, 2005, pH-responsive Carrier System Based on Carboxylic Acid Modified Mesoporous Silica and Polyelectrolyte for Drug Delivery. *Chem Mater*, 17:5999-6003. DOI 10.1021/cm051198v.
- Patel K, Angelos S, Dichtel WR, *et al.*, 2008, Enzyme-responsive Snap-top Covered Silica Nanocontainers. *J Am Chem Soc*, 130:2382-3. DOI 10.1021/ja0772086.
- Lin HM, Wang WK, Hsiung PA, *et al.*, 2010, Light-sensitive Intelligent Drug Delivery Systems of Coumarin-modified Mesoporous Bioactive Glass. *Acta Biomater*, 6:3256-63. DOI 10.1016/j.actbio.2010.02.014.
- Needham D, Dewhirst MW, 2001, The Development and Testing of a New Temperature-sensitive Drug Delivery System for the Treatment of Solid Tumors. *Adv Drug Deliv Rev*, 53:285-305. DOI 10.1016/S0169-409X(01)00233-2.
- Tang X, Li Q, Liang X, *et al.*, 2019, Inhibition of Proliferation and Migration of Tumor Cells Through Lipoic Acid-modified Oligoethylenimine-mediated p53 Gene Delivery. *New J Chem*, 43:2758-65. DOI 10.1039/c8nj05368e.
- Souris JS, Lee CH, Cheng SH, *et al.*, 2010, Surface Charge-mediated Rapid Hepatobiliary Excretion of Mesoporous Silica Nanoparticles. *Biomaterials*, 31:5564-74. DOI



- 10.1016/j.biomaterials.2010.03.048.
15. Ke CJ, Su TY, Chen HL, *et al.*, 2011, Smart Multifunctional Hollow Microspheres for the Quick Release of Drugs in Intracellular Lysosomal Compartments. *Angew Chem Int Ed*, 50:8086-9. DOI 10.1002/anie.201102852.
  16. Wang Y, Chen J, Liang X, *et al.*, 2017. An ATP-responsive Codelivery System of Doxorubicin and miR-34a to Synergistically Inhibit Cell Proliferation and Migration. *Mol Pharm*, 14:2323-32. DOI 10.1021/acs.molpharmaceut.7b00184.
  17. Lu S, Zhao F, Zhang Q, *et al.*, 2018. Therapeutic Peptide Amphiphile as a Drug Carrier with ATP-triggered Release for Synergistic Effect, Improved Therapeutic Index, and Penetration of 3D Cancer Cell Spheroids. *Int J Mol Sci*, 19:2773. DOI 10.3390/ijms19092773.
  18. Mo R, Jiang T, DiSanto R, *et al.*, 2014. ATP-triggered Anticancer Drug Delivery. *Nat Commun*, 5:3364. DOI 10.1038/ncomms4364.
  19. Wang GH, Huang GL, Zhao Y, *et al.*, 2016. ATP Triggered Drug Release and DNA co-delivery Systems Based on ATP Responsive Aptamers and Polyethylenimine Complexes. *J Mater Chem B*, 4:3832-41. DOI 10.1039/C5TB02764K.
  20. Zhang J, Wu D, Xing Z, *et al.*, 2015. N-Isopropylacrylamide-modified polyethylenimine-mediated p53 Gene Delivery to Prevent the Proliferation of Cancer Cells. *Colloids Surf B Biointerfaces*, 129:54-62. DOI 10.1016/j.colsurfb.2015.03.032.
  21. Xing Z, Gao S, Duan Y, *et al.*, 2015. Delivery of DNzyme Targeting Aurora Kinase A to Inhibit the Proliferation and Migration of Human Prostate Cancer. *Int J Nanomed*, 10:5715-27. DOI 10.2147/IJN.S90559.
  22. Leist M, Single B, Castoldi AF, *et al.*, 1997. Intracellular Adenosine Triphosphate (ATP) Concentration: A Switch in the Decision Between Apoptosis and Necrosis. *J Exp Med*, 185:1481-6. Doi 10.1084/jem.185.8.1481.
  23. Gribble FM, Loussouarn G, Tucker SJ, *et al.*, 2000. A Novel Method for Measurement of Submembrane ATP Concentration. *J Biol Chem*, 275:30046-9. DOI 10.1074/jbc.M001010200.
  24. Gorman MW, Feigl EO, Buffington CW, 2007. Human Plasma ATP Concentration. *Clin Chem*, 53:318-25. DOI 10.1373/clinchem.2006.076364.
  25. Zhang J, Wang Y, Chen J, *et al.*, 2017. Inhibition of Cell Proliferation through an ATP-responsive Co-delivery System of Doxorubicin and Bcl-2 siRNA. *Int J Nanomed*, 12:4721-32. DOI 10.2147/IJN.S135086.